Process Biochemistry 62 (2017) 161–168

Contents lists available at ScienceDirect

Process Biochemistry

journal homepage: www.elsevier.com/locate/procbio

Paper chip-based colorimetric sensing assay for ultra-sensitive detection of residual kanamycin

Na-Reum Ha[1], In-Pil Jung[1], Sang-Heon Kim, A-Ru Kim, Moon-Young Yoon*

Department of Chemistry and Research Institute of Natural Sciences, Hanyang University, Seoul 04763, Republic of Korea

ARTICLE INFO

Keywords:
Kanamycin
ssDNA aptamer
Gold nanoparticle
Paper chip
Colorimetric sensing assay

ABSTRACT

Kanamycin, an aminoglycoside antibiotic, is extensively used to treat bacterial infections by interrupting protein synthesis. Overuse of kanamycin can lead to undesirable outcomes such as antibiotic resistance in humans. Thus, a precise detection strategy for monitoring kanamycin in animal-derived foods is strongly required.

In this study, a novel paper chip-based label-free, simple sensing assay was developed. Gold nanoparticles for colorimetric assays were synthesized and characterized, and the paper chip pattern was printed using a wax printer. Through the colorimetric sensing assay on the paper chip, kanamycin was detected at levels as low as 3.35 nM (1.95 ppb) by the naked eye and using RGB color analysis techniques. In addition, this technique was also used for detection of kanamycin in milk samples. Compared to other detection systems, the use of the presented colorimetric detection system renders further analysis unnecessary. To our knowledge, this is the first report of colorimetric detection of kanamycin using the paper chip system. This simple, equipment-free, rapid, and ultra-sensitive paper chip-based kanamycin detection system provides superior field applicability for the monitoring of food and environmental safety.

1. Introduction

Kanamycin, an aminoglycoside bacterial antibiotic, is widely used in veterinary medicine for treating and preventing microbial infections, such as mastitis, pneumonia, and bacillary diarrhea [1,2]. Kanamycin contains Kanamycin A as the primary active component and only small amounts of structurally related components such as Kanamycin B and C [1]. However, an overuse of antibiotics can cause great problems for human health and environmental safety. Generally, the phenomenon of antibiotic abuse includes induction of bacterial resistance and other side effects, such as hearing loss, renal toxicity, and allergic reactions [2]. Therefore, organizations from different countries have set a maximum residue limit (MRL) for kanamycin in foodstuffs coming from animals treated with veterinary medicines or are exposed to biocidals, where a highly sensitive and selective technique for kanamycin detection in real samples is required. In particular, the Korea Food and Drug Administration (KFDA) fixed the MRL of kanamycin in milk to 0.1 ppm (0.1 mg/kg), and the European Union (EU) has established an MRL of 0.15 ppm (0.15 mg/kg) for milk [1,3,4]. Generally, analytical methods for kanamycin include high-performance liquid chromatography (HPLC) [5], and gas chromatography-mass spectrometry (GC–MS) [6], which have benefits with respect to qualitative analysis. However, these methods require expensive and large equipment, professional operators, and are time-consuming [2,7]. Thus, a new strategy for simple and rapid kanamycin detection is needed, including colorimetric methods [8], fluorescent methods [4], and the use of electrochemical biosensors [9].

Aptamers are short single-stranded oligonucleotides (usually 20–80 bases) with a highly ordered tertiary structure that forms stable and specific complexes with various targets, including small molecules, proteins, and cells [10]. Aptamers are selected from 10^{12}–10^{15} combinatorial oligonucleotide libraries by *in vitro* SELEX (systematic evolution of ligands by exponential enrichment) [4]. Aptamers undergo crucial conformational changes upon target binding that provides superior flexibility in biosensor platform applications, with a high level of detection sensitivity and selectivity [11]. Thus, aptamers are widely used as significant molecular tools for diagnostics and therapeutics owing to advantages such as high binding affinity and specificity, easy production and modification, low cost, and immunogenicity [12].

Recently, paper chip-based bioanalytical tools have been

Abbreviations: GNP, gold nanoparticle; SELEX, systematic evolution of ligands by exponential enrichment; MRL, maximum residue limit; FRET, fluorescence resonance energy transfer; TEM, transmission electron microscope; LOD, limit of detection

* Corresponding author at: Department of Chemistry and Research Institute of Natural Sciences, Hanyang University, 222 Wangsimni-ro, Seongdong-gu, Seoul, 04763, Republic of Korea.

E-mail address: myyoon@hanyang.ac.kr (M.-Y. Yoon).

[1] These authors contributed equally to this work.

http://dx.doi.org/10.1016/j.procbio.2017.07.008
Received 18 April 2017; Received in revised form 28 June 2017; Accepted 13 July 2017
Available online 15 July 2017
1359-5113/

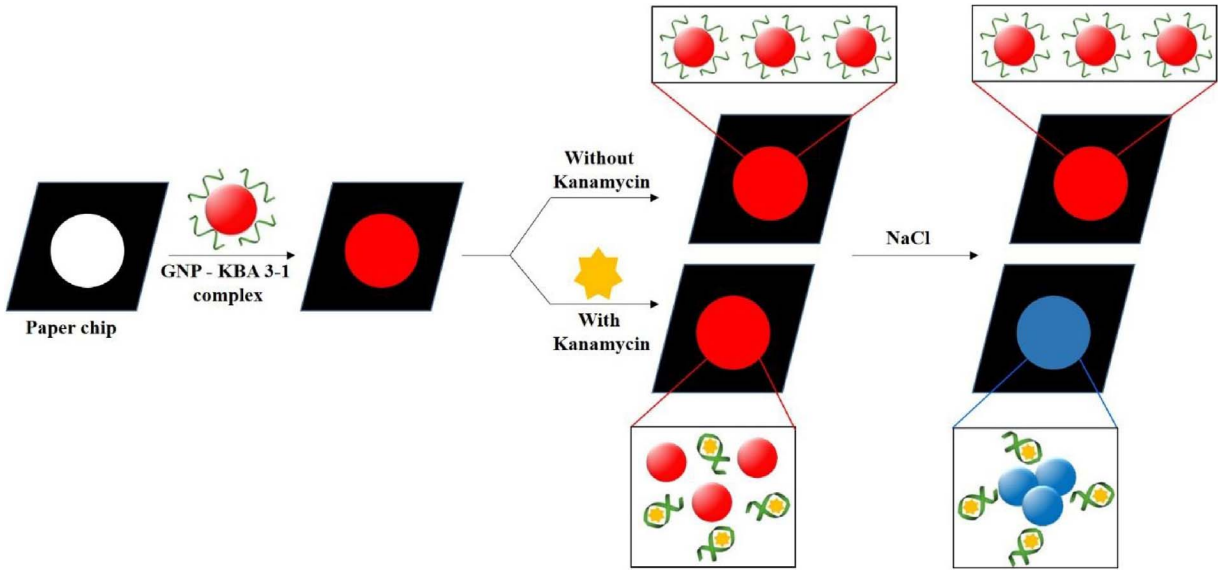

Fig. 1. A schematic representation of the paper chip-based colorimetric sensing assay for kanamycin detection.

extensively used in food safety analysis [13–15], molecular diagnostics [16–18], and environmental monitoring [19,20]. Paper chip-based sensors have many merits compared with traditional sensors, such as easy operation, low cost, portability, disposability, simple fabrication, and biocompatibility [21,22]. These remarkable properties of paper chip-based sensors have been integrated with various technologies including colorimetric [23,24] and fluorescence resonance energy transfer (FRET)-based fluorescent [25,26] methods.

Methods employing colorimetric paper chip sensors could provide simple techniques for visualizing a chemical reaction by the naked eye, with no affiliated instruments required. Thus, such techniques would be suitable for semi-quantitative and presence/absence analysis [27]. Gold nanoparticles (GNPs) have been widely used for sensing diverse biomolecules and harmful substances [28]. Their high surface to volume ratio, easy surface conjugation, and fascinating optical properties make GNPs valuable for highly sensitive and selective detection [29]. Colloidal GNPs generally exhibit a red or pink color due to a localized surface plasmon resonance that changes to purple-blue upon aggregation. Thus, control over the dispersion and aggregation of colloidal GNPs is an important feature of GNP-based colorimetric sensing platforms [30]. The colorimetric detection of biomolecules is possible due to the interaction between aptamers and GNPs.

In the present work, we developed a paper chip-based label-free, colorimetric sensing assay for the detection of Kanamycin A. In contrast with previous research, this study validates the possibility of achieving colorimetric detection of kanamycin on a paper chip. Quantification of RGB (Red Green Blue) color was used to digitize colorimetric images of assay performed on the paper chip. The detection system was also tested using animal-derived food, specifically milk. We present this as a novel simple strategy for monitoring the existence of kanamycin and other substances in animal-derived foodstuffs.

2. Materials and methods

2.1. Materials

Kanamycin sulfate (Kanamycin A) and ampicillin sodium salt were purchased from Biobasic (Markham, ON, Canada), and streptomycin sulfate, dihydrostreptomycin sesquisulfate, and tetracycline hydrochloride were obtained from Sigma (St. Louis, MO, USA). The 39-mer kanamycin-binding aptamer (KBA) 3-1 (5′-CGG AAG CGC GCC ACC CCA TCG GCG GGC GCG AAG CTT GCG-3′) and another reported reference aptamer, Ky 2 (5′-TGG GGG TTG AGG CTA AGC CGA-3′), were synthesized and purified using PAGE by Bioneer (Daejeon, Korea) [4,8]. Gold(III) chloride hydrate ($HAuCl_4$) and sodium citrate were purchased from Sigma (St. Louis, MO, USA). Lateral flow nitrocellulose (LFNC) 80 membrane for the paper chip was purchased from Nupore filtration systems (Ghaziabad, UP, India). All other chemicals were extra pure analytical grade and were obtained from commercial sources. Deionized water (18.2 MΩ cm^{-1}) from ELGA lab water purification system (High Wycombe, HP, UK) was used to prepare all aqueous solutions.

2.2. Apparatus

UV–vis absorption spectra were obtained using a SpectraMax M2 multi-mode microplate reader (Molecular Devices, Sunnyvale, CA, USA). High-magnification transmission electron microscopy (TEM) images were acquired using a JEOL JEM 2100F instrument (JEOL, Tokyo, Japan) at an accelerating voltage of 200 kV. The paper chip was prepared by wax printing using a commercial solid ink Xerox ColorQube 8870 printer (Xerox, Norwalk, CT, USA). All captured images were taken with a COOLPIX S8200 camera (Nikon, Tokyo, Japan).

2.3. Overview of GNP-based label-free colorimetric sensing assays on paper chips

Colloidal GNP solution shows strong absorbance of visible light at a specific wavelength, owing to the excitation of plasmons [31]. After treatment with high concentrations of a salt such as NaCl, citrate-coated GNPs aggregate and change color from wine red to purple blue [32]. However, adsorption of ssDNA aptamers onto GNPs can induce dispersion of GNPs and inhibit their aggregation. In this case, the dispersed GNPs can aggregate because of the binding interaction between ssDNA aptamer and kanamycin. In the presence of kanamycin, the ssDNA aptamer changes its conformation, where the tight structure of the aptamer-kanamycin complex blocks adsorption onto GNP surfaces. Furthermore, the specific interaction between kanamycin and its binding aptamer is stronger than the electrostatic interaction between the aptamer and GNPs [32]. Consequently, the presence of kanamycin induces detachment of the ssDNA aptamer from GNPs, and changes the GNP color from wine red to purple blue upon salt addition. The above colorimetric assay was then adapted to the paper chip system (Fig. 1). Wax printing is rapid, inexpensive, and particularly well suited to paper chip production [33]. The wax was used for constructing a hydrophobic barrier on the nitrocellulose membrane. The results were analyzed by

monitoring the color change visible with the naked eye and the RGB color intensity.

2.4. Synthesis and characterization of size-tunable gold nanoparticles

The GNPs were prepared from citrate reduction of $HAuCl_4$ [34]. Prior to use, all glassware was thoroughly cleaned with aqua regia (3:1 concentrated hydrochloric acid (HCl): concentrated nitric acid (HNO_3)), rinsed in triply distilled H_2O and oven-dried. The size-controlled synthesis of GNPs was performed using different concentrations of sodium citrate [32]. A 50 mL aqueous solution of $HAuCl_4$ (1 mM, 0.02 g/50 mL) was refluxed for 15 min in a 500 mL round bottom flask with rapid stirring. Different concentrations of sodium citrate solution, *i.e.*, 10 mL of 40 mM (0.1 g/10 mL), 10 mM (0.025 g/10 mL), and 6 mM (0.015 g/10 mL), were prepared for synthesis of 14 nm GNP-A, 21 nm GNP-B, and 27 nm GNP-C respectively. The prepared gold solutions (1 mM) were heated to boiling point on a plate cum magnetic stirrer. After 20 min of boiling, each of the above mentioned sodium citrate solutions were quickly added to the boiling $HAuCl_4$ solutions and continuously stirred for an additional 10 min. After boiling, the color of the solution changed from yellow to white, and then to black. Boiling was continued until different colors depending on size were obtained. After synthesis, the three types of size-tunable GNP solutions were stored at 4 °C for further use. The different types of GNPs were characterized in terms of morphology, size, and shape, and the maximum wavelength (λ_{max}) by transmission electron microscopy (TEM) and ultraviolet-visible (UV–vis) spectroscopy, respectively. The mean particle size of GNPs was calculated using Image J software and the Gaussian fitting model in the Origin program.

2.5. Colorimetric kanamycin detection procedure

In a 96-well plate, the volume of each colorimetric sensing system was fixed at 200 μL and the GNP concentration was a UV absorbance value of approximately 1.0. First, 180 μL of citrate-coated GNPs (4.57 nM final concentration) were incubated with 10 μL of the 39-mer kanamycin binding aptamer (KBA 3-1, 1 μM) for 15 min at room temperature with mild shaking. Then, 10 μL of different concentrations of kanamycin (0–860 nM) was added to each well for 15 min. After the addition of 20 μL of NaCl (68.18 mM final concentration), the change in color was visualized by the naked eye and spectra were produced using the SpectraMax M2 multi-mode microplate reader (Molecular Devices, Sunnyvale, CA, USA). Finally, this detection strategy was applied to the paper chip-based detection system.

2.6. Colorimetric sensing assay sensitivity and selectivity

The sensitivity of the GNP-based colorimetric sensing assay was tested using various kanamycin concentrations. The limit of detection (LOD) was calculated using Eq. (1) and selectivity was analyzed in the presence of streptomycin, dihydrostreptomycin, tetracycline, and ampicillin (500 nM final concentration) using the same procedure described for kanamycin.

$$LOD = 3 \times \sigma/N \quad (1)$$

Where σ is the relative standard deviation of the blank, and N is the slope of the fitted line.

2.7. Preparation of the paper-based chip

The paper-based chip was prepared using the same protocol used in a previous study [35]. Using a commercial solid ink Xerox ColorQube 8870 printer, the LFNC 80 membrane was printed with a mask containing single circular wax-free regions (hydrophilic regions) that were 4 mm in diameter and surrounded by dark regions (hydrophobic regions). The printed paper was heated to allow the melting of wax and its penetration through the paper to form isolated, hydrophilic, unprinted regions surrounded by hydrophobic barriers. Each hydrophilic region was used independently and is henceforth referred to as a 'test zone'. The paper chip was stored in a desiccator until further use.

2.8. Detection of kanamycin on the paper chip

The assay protocol was the same described in the 'Materials and methods' Section 2.4. First, 18 μL of citrate-coated GNPs (4.57 nM final concentration) were incubated with 1 μL of the 39-mer kanamycin binding aptamer (KBA 3-1, 1 μM) for 15 min at room temperature with mild shaking. The GNP-KBA 3-1 mixture (19 μL) was added to the test zone of the paper chip and dried, followed by addition of the kanamycin standard (10 μL). After drying completely, 20 μL of salt was added to monitor the color change.

2.9. Analysis of kanamycin in real samples

To investigate the practicability of the colorimetric sensing assay, the detection method was further applied to the detection of kanamycin in milk. First, milk was briefly pretreated to remove various proteins using acetic acid precipitation as described previously [4]. Using the standard addition method, artificially contaminated milk was generated by spiking kanamycin into kanamycin-free pretreated milk (4, 8, and 12 nM final concentration). The label-free colorimetric assay was then carried out on the paper chip as described above.

2.10. Imaging and image analysis

All images were taken with a camera (COOLPIX S8200, Nikon), and the captured images were used without any modification. For analysis of the RGB color space, each image was opened in the Image J program and separated into red, green, and blue channels. The average intensity of each of the channels was calculated for the test zone and the values were exported to MS excel [35]. In this colorimetric reaction, the red color dramatically changed to blue, thus, the value of the red channel (100/R) was used for the quantitative analysis of color intensity.

3. Results and discussion

3.1. Characterization of GNPs

GNPs of different sizes were synthesized using different concentrations of sodium citrate [36]. The optical properties of the synthesized GNPs of three different sizes were characterized in terms of size and shape, and maximum wavelength (λ_{max}) by TEM and UV–vis spectroscopy, respectively.

Upon increasing the sodium citrate concentration in the reaction mixture from 6 mM to 40 mM, there was a blue shift in the maximum wavelength of the synthesized GNPs from 530 nm to 520 nm (Fig. 2A). Furthermore, the different GNP samples were also analyzed structurally by TEM (Fig. 2B–D). The morphology of the synthesized GNPs was homogeneous and spherical. However, as the size of GNPs increased, the shape of the GNPs was changed from spherical to other shapes such as triangular. The variation in the size and shape of GNPs indicates that the GNP synthesis process was well-controlled by varying the sodium citrate concentration. Different nucleation steps caused by regulating the sodium citrate concentration during GNP formation induced changes in the size, shape, and optical properties of the GNPs, as found previously [37,38]. Using Image J and the Gaussian fitting model in the Origin program, the mean particle size was calculated to be 14.14 ± 3.55 nm (GNP-A), 21.68 ± 0.43 nm (GNP-B), and 27.28 ± 0.57 nm (GNP-C). The final concentration of the three different sizes of synthetic GNPs was calculated as 11.43 nM (6.88×10^{15} particles/L), 11.02 nM (6.63×10^{15} particles/L), and 11.77 nM

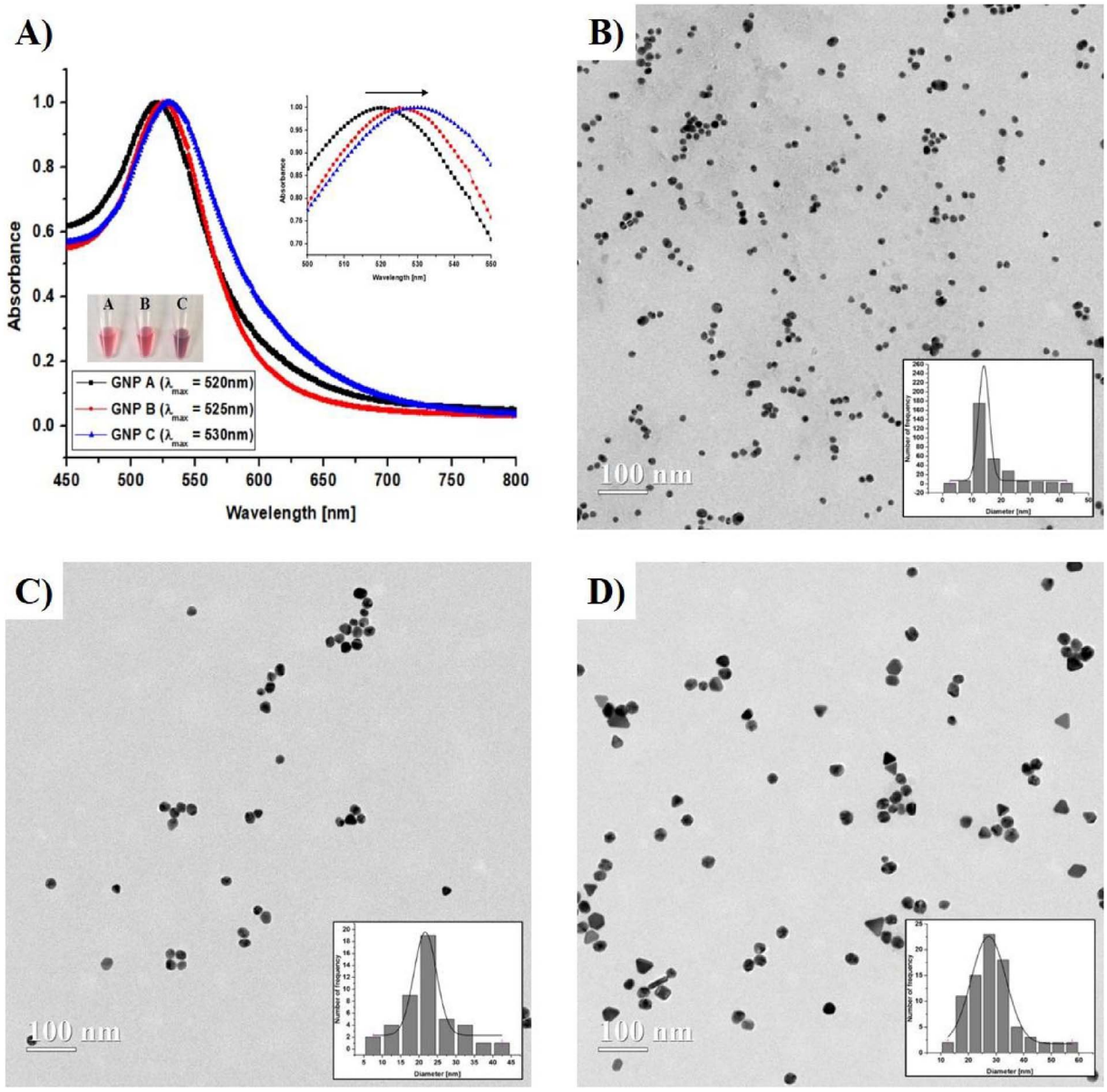

Fig. 2. Characterization of three types of synthetic gold nanoparticles (GNPs). (A) UV–vis spectra of synthetic GNPs (GNP-A, B, C). The concentration of each of the GNPs is approximately 0.23 mg/mL. (B-D) TEM images and histograms of synthetic GNP: (B) GNP-A: 14.14 ± 3.55 nm, (C) GNP-B: 21.68 ± 0.43 nm, (D) GNP-C: 27.28 ± 0.57 nm. Scale bars are 100 nm.

(7.09×10^{15} particles/L), respectively.

3.2. Optimization of conditions

The following experimental factors in the label-free colorimetric sensing assay were optimized against the three types of GNPs: the concentration of (i) GNP, (ii) NaCl, and (iii) KBA 3-1. The results are shown in Fig. S1. Assessing the concentration of GNPs is essential to confirm visual detection easily and quickly. As shown in Figs. S1A, D, and G, the concentration of each of the GNPs was analyzed by UV–vis spectroscopy. The color of the GNPs should make the differentiation between each condition simple, where a suitable aptamer concentration is needed to protect the GNPs from aggregation and thereby exhibit good sensitivity. Thus, GNP samples with an absorbance of 1.0 at 520 nm equating to calculated concentrations of 4.57, 4.52, and 4.57 nM for GNP-A, GNP-B, and GNP-C, respectively, were used for further reactions.

Sodium ions can induce the aggregation of citrate-coated GNPs. To optimize the sodium ion concentration for aggregation, we added different concentrations of NaCl (0–90 mM final concentration) (Fig. S1B, E, and H). The sodium concentration required for complete aggregation of GNP-B and C (45.44 mM) was less than that for GNP-A (68.18 mM). Therefore, the results indicate that GNPs with a larger size aggregate more easily.

Next, the optimum KBA 3-1 concentration was determined. The ssDNA aptamer was previously shown to uncoil sufficiently to expose its bases, allowing for strong chemical bonding interactions between nitrogen atoms in the DNA bases and GNP surfaces. Thereby, adsorbed DNA protect GNPs against salt-induced aggregation [39]. In the present experiment, various concentrations of KBA 3-1 were incubated with each of the GNPs and 20 μL NaCl was then added. More than 1 μM of KBA 3-1 was adsorbed on GNP-A surfaces, displaying stability against salt-induced aggregation (Fig. S1C). However, 10 μM of KBA 3-1 was required for thorough adsorption onto GNP-B and C surfaces (Fig. S1F and I). It was previously reported that increased detection sensitivity against salt can be caused by lower aptamer adsorption concentrations [40] and an excessive amount of aptamers results in lowered detection sensitivity owing to competitive interaction dynamics among aptamers,

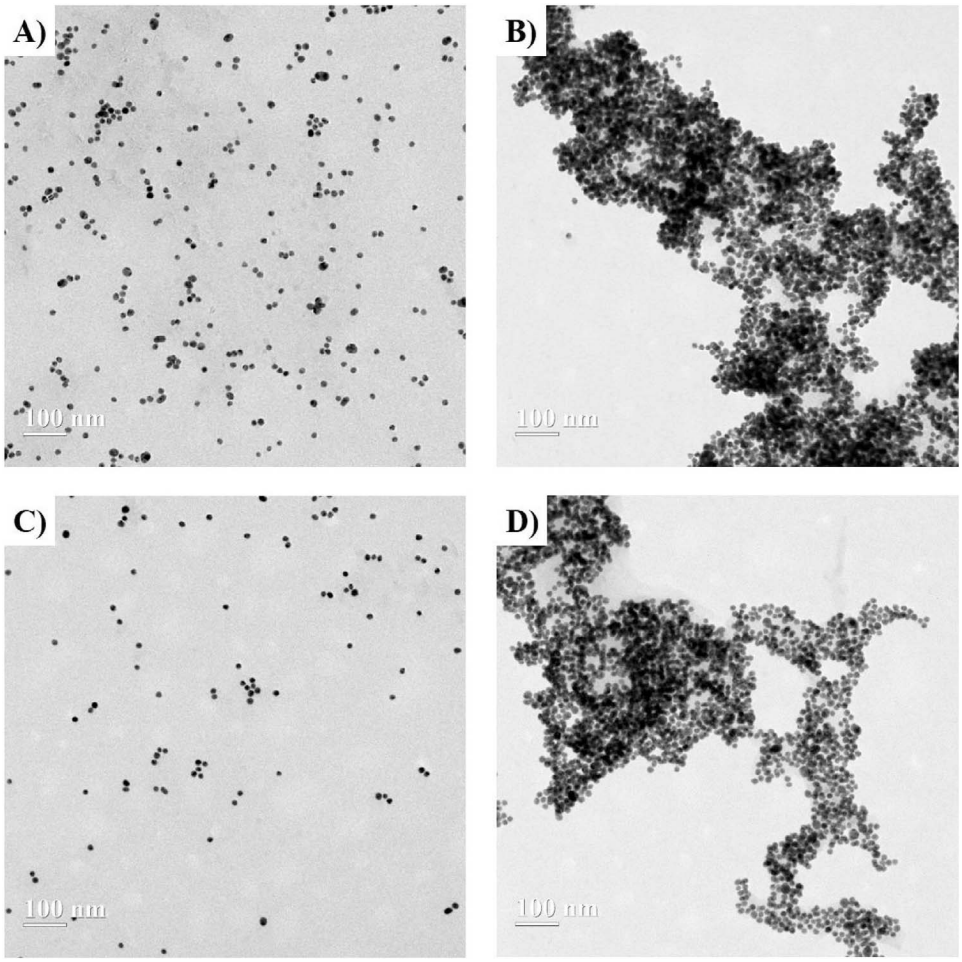

Fig. 3. TEM images of the GNP solutions treated with different materials. (A) Blank GNP, (B) GNP + 68 mM NaCl, (C) GNP + 1 μM KBA 3–1 + 68 mM NaCl, and (D) GNP + 1 μM KBA 3–1 + 500 nM kanamycin + 68 mM NaCl.

GNPs, and targets [41]. A high KBA 3-1 concentration leads to low detection sensitivity and cost ineffectiveness for aptamer production, and thus, only the smallest GNP, GNP-A (14 nm diameter), was selected for further experiments. Consequently, 4.57 nM GNP-A, 68.18 mM NaCl, and 1 μM KBA 3-1 were subsequently used in colorimetric assays.

3.3. TEM verification of the colorimetric assay

In order to validate the principles behind the sensing assay, the dispersion and aggregation of GNPs was evaluated by TEM. Fig. 3 shows the image of the GNP solution treated with various materials: (i) free GNPs, (ii) GNPs with NaCl, (iii) KBA 3-1 adsorbed by GNPs (GNP-KBA 3-1) with NaCl, and (iv) incubation of kanamycin with GNP-KBA 3-1 and then the addition of NaCl. The free GNPs were well dispersed with an average particle diameter of 14 nm (Fig. 3A). The addition of NaCl induced complete aggregation of the GNPs (Fig. 3B). In contrast, incubation of KBA 3-1 with the GNP solution, creating GNP-KBA 3-1, retained the dispersed state despite NaCl treatment (Fig. 3C). When 500 nM of kanamycin was added to the GNP-KBA 3-1 complex, most of the GNPs aggregated upon treatment with NaCl (Fig. 3D). This phenomenon corresponded with the principle of this colorimetric assay. The native GNP was completely aggregated by NaCl, whereas GNPs dispersed by adsorption of the ssDNA aptamer maintained their stability against salt treatment. Although KBA 3-1 has a relatively large number of G bases, KBA 3-1 does not have the G-quadruplex structure found in G-rich sequences (data is not shown). Before KBA 3-1 reacts with its target, kanamycin, KBA 3-1 remains as a flexible ssDNA with a random coil structure [42]. Thus, the random coil structure of the ssDNA aptamer is unlikely to inhibit effective adsorption onto GNP surfaces. The ssDNA aptamer was adsorbed onto the surface of GNPs through non-covalent interactions between the exposed nitrogen bases and the GNPs. This results in the addition of negative charges to the GNPs, increasing repulsion, and stabilizing the GNPs [39,43]. The ssDNA aptamers that are adsorbed onto the GNPs was detached because of conformational changes induced by the kanamycin-aptamer complex, GNP-KBA 3-1, generating free GNPs that are easily aggregated by the addition of salt.

3.4. Development of the label-free colorimetric sensing assay for kanamycin detection

After optimizing the experimental conditions, we determined the limit of detection for kanamycin. Fig. 4A presents the UV–vis absorbance spectra of the GNPs in the presence of various kanamycin concentrations (0–860 nM). By the kanamycin treatment, the absorbance at 520 nm gradually decreased and showed a red-shift with a steadily increased absorbance at 650 nm. The linear relation between the ratio value of absorbance (A_{650}/A_{520}) and the kanamycin concentration was obtained in the range from 3.35 nM to 53.75 nM ($y = 0.011x + 0.3484$, $R^2 = 0.9663$), and the limit of detection (LOD) was about 3.35 nM (Fig. 4B). In order to compare the detection sensitivity with other kanamycin binding aptamers, the Ky 2 reference aptamer was also tested. As shown in Fig. S2A and B, the LOD was ~26.8 nM, similar to values obtained in previous research (LOD = 25 nM) [8]. Consequently, in the present research, the KBA 3-1 LOD displayed ~8-fold more sensitivity than was previously reported for the Ky 2 aptamer. KBA 3-1 and Ky 2 had a similar binding affinity for kanamycin (92.3 and 78.8 nM respectively). However, KBA 3-1 displayed greater sensitivity toward kanamycin than Ky 2. For Ky 2, a concentration of 4 μM was required to be adsorbed completely on GNPs surfaces and stabilized

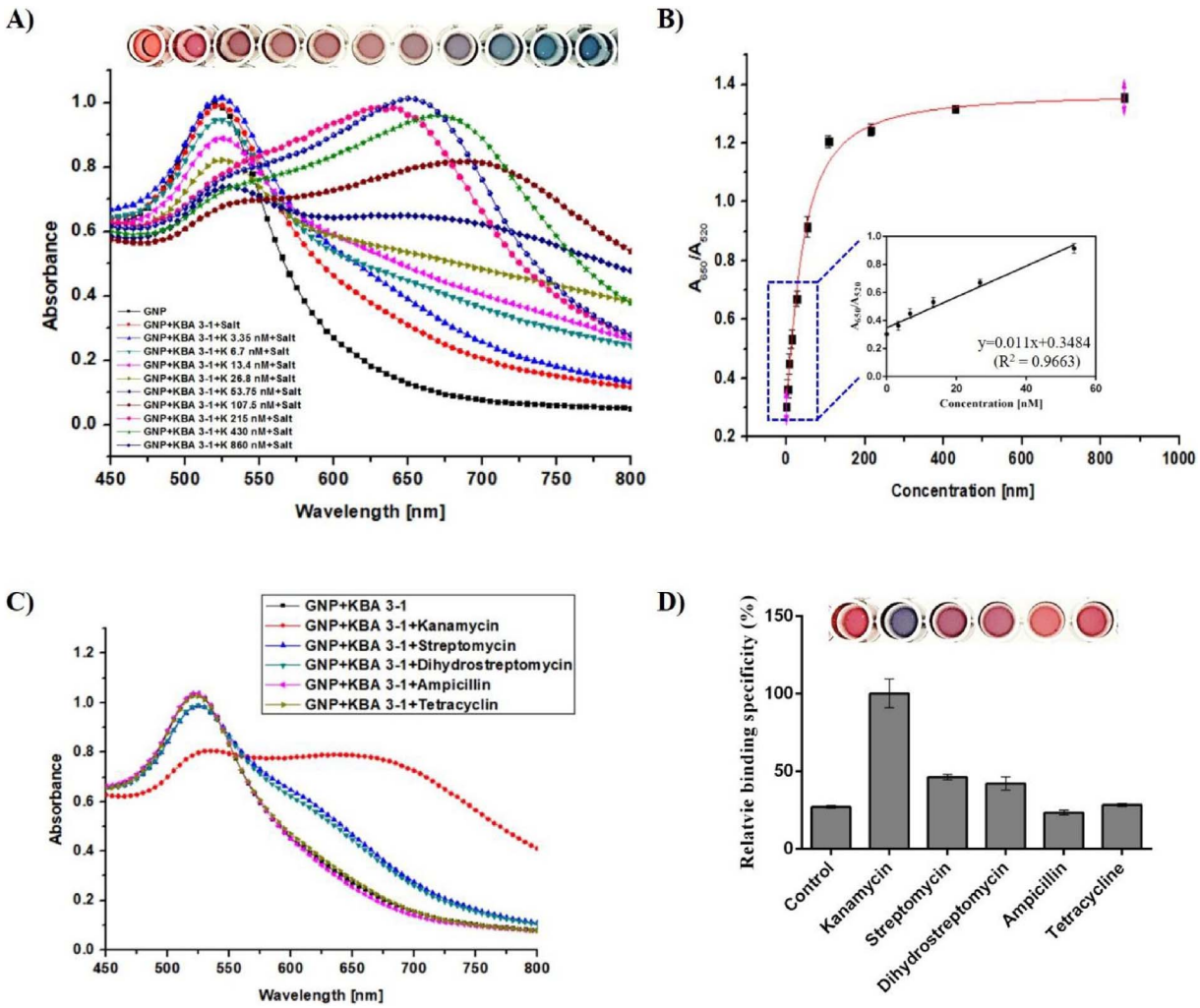

Fig. 4. Sensitivity (A, B) and selectivity (C, D) of the colorimetric sensing assay for kanamycin detection. (A) UV–vis absorbance spectra and visual color changes of GNP in the presence of different concentrations of kanamycin (0, 3.35, 6.7, 13.4, 26.8, 53.75, 107.5, 215, 430, and 860 nM). (B) The absorbance ratio (A_{650}/A_{520}) of GNP *versus* different concentrations of kanamycin. The linear correlation of the absorbance ratio (A_{650}/A_{520}) for GNP in the range of 3.35–53.75 nM. Errors bars were calculated from three experiments. (C) UV–vis absorbance spectra of GNP in the presence of 500 nM antibiotics (kanamycin, streptomycin, dihydrostreptomycin, ampicillin, tetracycline). (D) Relative binding specificity of the colorimetric sensing assay.

the GNPs. As discussed in Section 3.2, a higher aptamer adsorption concentration induces decreased sensitivity [40,41].

To investigate the selectivity of the label-free colorimetric sensing assay, streptomycin, dihydrostreptomycin, ampicillin, and tetracycline (500 nM) were selected for testing. As illustrated in Fig. 4C and D, the proposed system had higher binding specificity for kanamycin than the other tested antibiotics that displayed a much lower signal (A_{650}/A_{520}). Furthermore, a selectivity test using Ky 2 was also performed. Figs. S2C and D show that the Ky 2 aptamer had less specificity for kanamycin than KBA 3-1. More specifically, the colorimetric sensing assay using Ky 2 detected kanamycin and dihydrostreptomycin similarly (95%, Fig. S2D), whereas KBA 3-1 showed a dominant detection signal for kanamycin only. Therefore the detection specificity of KBA 3-1 for kanamycin is higher because KBA 3-1 could detect kanamycin more clearly than other antibiotics than compared to the Ky 2 results.

3.5. Paper chip-based colorimetric detection of kanamycin

The analytical performance of the label-free colorimetric kanamycin sensing assay on the paper chip was further investigated. Prior to the experiment, the wax pattern for a single circle test zone was printed on a LFNC 80 membrane (Fig. S3). As shown in Fig. 5A, the color on each paper chip changed gradually from red to dark blue, and the 100/R value increased when the kanamycin concentration increased from 3.35 nM to 860 nM. The color exhibited by this reaction caused the maximum change in the red channel intensity as opposed to green or blue. Therefore, the red channel from the RGB value was used for further analysis (Fig. S4). The average 100/R peak values from triplicate showed a strong linear correlation with the kanamycin concentration ranging from 3.35 nM to 13.4 nM. The linear equation was calibrated as $y = 0.02675x + 0.5616$ ($R^2 = 0.9651$). Thus, the LOD for kanamycin was 3.35 nM, corresponding with the above result. Furthermore, the paper chip-based colorimetric sensing assay using KBA 3-1 showed remarkable detection sensitivity for kanamycin compared to an aptamer reported previously for colorimetric detection (Table 1). This suggested assay using KBA 3-1 can be visualized by the naked eye, having multiple advantages, including ultra-sensitive, rapid, simple, and cost-effective detection of kanamycin. The total reaction time was just 30 min.

A selectivity test was also performed on the paper chip (Fig. 5B). Results showed a similar detection tendency as in the above result and that reported in previous studies using fluorescent methods [4]. This confirms that the high selectivity of this sensor system was attributed to the high specificity of KBA 3-1.

This paper chip colorimetric assay is more efficient for quickly analyzing yes/no or semi-quantitative results. However, it is possible to

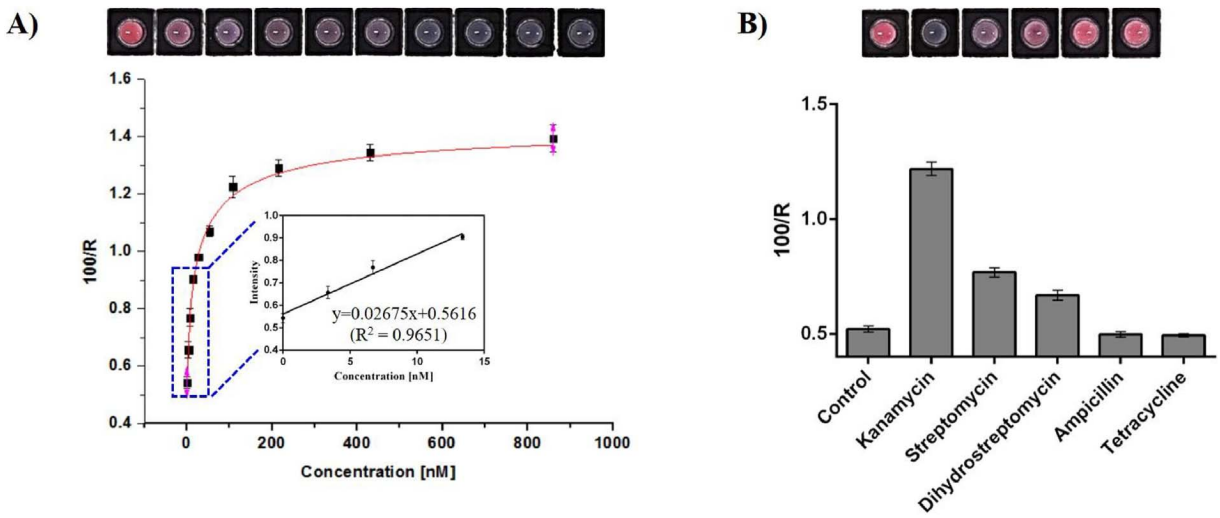

Fig. 5. Sensitivity and selectivity of the paper chip-based colorimetric sensing assay. (A) RGB color intensity and visual color change of GNP in the presence of different concentrations of kanamycin (0, 3.35, 6.7, 13.4, 26.8, 53.75, 107.5, 215, 430, and 860 nM). The linear correlation of the absorbance ratio (A_{650}/A_{520}) for GNP in the range of 3.35–13.4 nM. (B) RGB color intensity of GNP in the presence of 500 nM antibiotics (kanamycin, streptomycin, dihydrostreptomycin, ampicillin, tetracycline).

perform a quantitative analysis *via* the use of a color and image analysis software (*e.g.*, Image J program). The sensitivity and selectivity results for the colorimetric assays performed on the paper chip (RGB image analysis) and in solution state (UV–vis spectroscopy) were almost identical. This indicates that the colorimetric assay performed on the paper chip could become a well-established system for kanamycin detection and could substitute the spectroscopy-based measurement technique with an equipment-free method.

3.6. Paper chip-based colorimetric detection of kanamycin in milk

Finally, in order to evaluate the feasibility of the suggested colorimetric sensing assay for practical applications in testing animal products, the detection of kanamycin was carried out in milk. Two different milk samples were pretreated with acetic acid for protein removal, and three known concentrations of kanamycin (4, 8, 12 nM) were added to the pretreated milk samples (Fig. S5). As shown in Table 2, the mean recoveries of the spiked kanamycin samples were between 99.03 and 108.69%, with a relative standard deviation (RSD) range of 2.09–8.83%.

With respect to the maximum residue level (MRL) of kanamycin in milk (0.1 ppm, 171 nM) established by the KFDA, the proposed platform could efficiently detect kanamycin at levels much lower than the MRL. These results indicate that further detection of kanamycin in other animal product-based samples could be possible using the described sensing assay. In particular, the paper chip-based colorimetric detection of kanamycin could provide a simple strategy to obtain results within 30 min, excluding the same preparation steps required for qualitative as well as quantitative analysis.

We recently reported the results of a reduced graphene oxide (RGO)-based fluorescent aptasensor assay for kanamycin detection [4]. Compared with this fluorescent assay, the colorimetric sensing assay enables an instrument-free readout using the naked eye, which is useful in resource limited settings (RLS) without a laboratory infrastructure [44]. Thus, the development of paper chip formats for biosensing and point-of-care monitoring of food and environmental safety could be easily achieved on-site in the absence of laboratory instruments.

Table 2
Detection of kanamycin in spiked milk samples.

Samples	Added (nM)	Detected (nM)[a]	Recovery (%)	RSD (%, n = 3)
Milk 1	4	4.15	103.86	5.33
	8	7.92	99.03	4.61
	12	12.20	102.58	3.87
Milk 2	4	4.34	108.69	8.83
	8	7.99	99.92	4.67
	12	12.42	101.78	2.09

[a] Mean values of three experiments.

4. Conclusion

In the present study, a novel paper chip-based colorimetric sensing assay was developed for the detection of kanamycin. In order to assess the monitoring of kanamycin in the field, this proposed system also carried out on a nitrocellulose membrane-based paper chip. The LOD of kanamycin determined using the KBA 3-1-based sensing platform was estimated to be 3.35 nM (1.95 ppb). This value is ~8-fold greater than the kanamycin detection sensitivity reported for the Ky 2 aptamer-based detection method (LOD = 26.8 nM). The suggested strategy provided precise kanamycin detection in standard milk samples within 30 min (excluding the time taken for sample preparation, such as pretreatment of milk samples). We believe that this novel paper chip-based colorimetric sensing assay is a convenient, simple, low sample consumption, and rapid diagnostic platform for monitoring of kanamycin in equipment-free fields.

Table 1
Comparison of various colorimetric kanamycin detection methods.

Strategy	Linear range (M)	Detection limit (M)	References
Unmodified GNPs and ssDNA aptamer (Ky 2)	–	25×10^{-9}	[8]
Unmodified AgNPs and ssDNA aptamer (Ky 2)	8.58×10^{-8}–1.03×10^{-6}	4.6×10^{-9}	[45]
Unmodified GNPs and ssDNA aptamer (Ky 2) in multiplex detection	–	171.6×10^{-9}	[46]
Unmodified GNPs and ssDNA aptamer (KBA 3-1)	3.35×10^{-9} –13.40×10^{-9}	3.35×10^{-9}	This study

Acknowledgement

This work was supported by the Agricultural Biotechnology Development Program, Ministry of Agriculture, Food and Rural Affairs, Republic of Korea (314013-3).

Appendix A. Supplementary data

Supplementary data associated with this article can be found, in the online version, at http://dx.doi.org/10.1016/j.procbio.2017.07.008.

References

[1] Y. Wang, M. Zou, Y. Han, F. Zhang, J. Li, X. Zhu, Analysis of the kanamycin in raw milk using the suspension array, J. Chem. 2013 (2013) 1–4.
[2] Y. Wang, T. Ma, S. Ma, Y. Liu, Y. Tian, R. Wang, Y. Jiang, D. Hou, J. Wang, Fluorometric determination of the antibiotic kanamycin by aptamer-induced FRET quenching and recovery between MOS2 nanosheets and carbon dots, Microchim. Acta 184 (2017) 203–210.
[3] C.M. Lim, B.H. Cho, G.S. Chung, S.W. Son, Determination of aminoglycosides in milk by liquid chromatography with tandem mass spectrometry, Kor. J. Vet. Public Health 36 (2012) 121–130.
[4] N.R. Ha, I.P. Jung, I.J. La, H.S. Jung, M.Y. Yoon, Ultra-sensitive detection of kanamycin for food safety using a reduced graphene oxide-based fluorescent aptasensor, Sci. Rep. 7 (2017) 1–10.
[5] B. Blanchaert, E.P. Jorge, P. Jankovics, E. Adams, A.V. Schepdael, Assay of kanamycin A by HPLC with direct UV detection, Chromatographia 76 (2013) 1505–1512.
[6] N. Isoherranen, S. Soback, Chromatographic methods for analysis of aminoglycoside antibiotics, J. AOAC Int. 82 (1999) 1017–1045.
[7] C.S. Pundir, B. Batra, Determination of β-ODAP by various methods with special emphasis on biosensors: a mini-review, Process Biochem. 50 (2015) 2078–2087.
[8] K.M. Song, M. Cho, H. Jo, K. Min, S.H. Jeon, T. Kim, M.S. Han, J.K. Ku, C. Ban, Gold nanoparticle-based colorimetric detection of kanamycin using a DNA aptamer, Anal. Biochem. 415 (2011) 175–181.
[9] Y. Zhu, P. Chandra, K.M. Song, C. Ban, Y.B. Shim, Label-free detection of kanamycin based on the aptamer-functionalized conducting polymer/gold nanocomposite, Biosens. Bioelectron. 36 (2012) 29–34.
[10] J. Zhang, B. Liu, H. Liu, X. Zhang, W. Tan, Aptamer-conjugated gold nanoparticles for bioanalysis, Nanomedicine 8 (2013) 983–993.
[11] S. Song, L. Wang, J. Li, J. Zhao, C. Fan, Aptamer-based biosensors, Trends Anal. Chem. 27 (2008) 108–117.
[12] N.R. Ha, S.C. Lee, J.W. Hyun, M.Y. Yoon, Development of inhibitory ssDNA aptamers for the FtsZ cell division protein from citrus canker phytopathogen, Process Biochem. 51 (2016) 24–33.
[13] S.M. Zakir Hossain, R.E. Luckham, M.J. McFadden, J.D. Brennan, Reagentless bidirectional lateral flow bioactive paper sensors for detection of pesticides in beverage and food samples, Anal. Chem. 81 (2009) 9055–9064.
[14] M. Li, R. Cao, A. Nilghaz, L. Guan, X. Zhang, W. Shen, Periodic-table-style paper device for monitoring heavy metals in water, Anal. Chem. 87 (2015) 2555–2559.
[15] Y. Zhang, P. Zuo, B.C. Ye, A low-cost and simple paper-based microfluidic device for simultaneous multiplex determination of different types of chemical contaminants in food, Biosens. Bioelectron. 68 (2015) 14–19.
[16] J.T. Connelly, J.P. Rolland, G.M. Whitesides, Paper machine for molecular diagnostics, Anal. Chem. 87 (2015) 7595–7601.
[17] A.M. Foudeh, T.F. Didar, T. Veres, M. Tabrizian, Microfluidic designs and techniques using lab-on-a-chip devices for pathogen detection for point-of-care diagnostics, Lab Chip 12 (2012) 3249–3266.
[18] X. Mu, L. Zhang, S. Chang, W. Cui, Z. Zheng, Multiplex microfluidic paper-based immunoassay for the diagnosis of Hepatitis C virus infection, Anal. Chem. 86 (2014) 5338–5344.
[19] N.A. Meredith, C. Quinn, D.M. Cate, T.H. Reilly III, J. Volckens, C.S. Henry, Paper-based analytical devices for environmental analysis, Analyst 1141 (2016) 1874–1887.
[20] L.J. Sun, Q.M. Feng, Y.F. Yan, Z.Q. Pan, X.H. Li, F.M. Song, H. Yang, J.J. Xu, N. Bao, H.Y. Gu, Paper-based electroanalytical devices for *in situ* determination of salicylic acid in living tomato leaves, Biosens. Bioelectron 60 (2014) 154–160.
[21] M.Y. Hsu, C.Y. Yang, W.H. Hsu, K.H. Lin, C.Y. Wang, Y.C. Shen, Y.C. Chen, S.F. Chau, H.Y. Tsai, C.M. Cheng, Monitoring the VEGF level in aqueous humor of patients with ophthalmologically relevant disease via ultrahigh sensitive paper-based ELISA, Biomaterials 35 (2014) 3729–3735.
[22] H. Tao, L.R. Chieffo, M.A. Brenckle, S.M. Siebert, M. Liu, A.C. Strikwerda, K. Fan, D.L. Kaplan, X. Zhang, R.D. Averitt, F.G. Omenetto, Metamaterials on paper as a sensing platform, Adv. Mater. 23 (2011) 3197–3201.
[23] J.I. Hong, B.Y. Chang, Development of the smartphone-based colorimetry for multi-analyte sensing arrays, Lab Chip 14 (2014) 1725–1732.
[24] P. Liang, H. Yu, B. Guntupalli, Y. Xiao, Paper-based device for rapid visualization of NADH based on dissolution of gold nanoparticles, ACS Appl. Mater. Interfaces 7 (2015) 15023–15030.
[25] M. He, Z. Liu, Paper-based microfluidic device with upconversion fluorescence assay, Anal. Chem. 85 (2013) 11691–11694.
[26] H. Li, X. Fang, H. Cao, J. Kong, Paper-based fluorescence resonance energy transfer assay for directly detecting nucleic acids and proteins, Biosen. Bioelectron. 80 (2016) 79–83.
[27] W. Chen, X.F. Hua, H. Cao, J. Kong, A simple paper-based colorimetric device for rapid mercury (II) assay, Sci. Rep. 6 (2016) 1–7.
[28] P. Nath, R.K. Arun, N. Chanda, A paper based microfluidic device for the detection of arsenic using a gold nanosensor, RSC Adv. 4 (2014) 59558–59561.
[29] F.M. Mazar, M. Alijanianzadeh, A. Molaeirad, P. Heydari, Development of novel glucose oxidase immobilization on Graphene/Gold nanoparticles/Poly neutral red modified electrode, Process Biochem. 56 (2017) 71–80.
[30] E. Priyadarshini, N. Pradhan, Gold nanoparticles as efficient sensors in colorimetric detection of toxic metal ions: a review, Sens. Actuators B Chem. 238 (2017) 888–902.
[31] X. Huang, M.A. El-Sayed, Gold nanoparticles: optical properties and implementations in cancer diagnosis and photothermal therapy, J. Adv. Res. 1 (2010) 13–28.
[32] S. Wang, S. Gao, S. Sun, Y. Yang, Y. Zhang, J. Liu, Y. Dong, H. Su, T. Tan, A molecular recognition assisted colorimetric aptasensor for tetracycline, RSC Adv. 6 (2016) 45645–45651.
[33] L. Liang, M. Su, L. Li, F. Lan, G. Yang, S. Ge, J. Yu, X. Song, Aptamer-based fluorescent and visual biosensor for multiplexed monitoring of cancer cells in microfluidic paper-based analytical devices, Sens. Actuators B Chem. 229 (2016) 347–354.
[34] R. Lévy, N.T.K. Thanh, R.C. Doty, I. Hussain, R.J. Nichols, D.J. Schiffrin, M. Brust, D.G. Fernig, Rational and combinatorial design of peptide capping ligands for gold nanoparticles, J. Am. Chem. Soc. 126 (2004) 10076–10084.
[35] S. Lathwal, H.D. Sikes, Assessment of colorimetric amplification methods in a paper-based immunoassay for diagnosis of malaria, Lab Chip 16 (2016) 1378–1382.
[36] P.R. Sahoo, P. Singh, Size tunable gold nanoparticle and its characterization for labeling application in animal health, Vet. World 7 (2014) 1010–1013.
[37] C. Li, D. Li, G. Wan, J. Xu, W. Hou, Facile synthesis of concentrated gold nanoparticles with low size-distribution in water: temperature and pH controls, Nanoscale Res. Lett. 6 (2011) 1–10.
[38] K. Alaqad, T.A. Saleh, Gold and silver nanoparticles: synthesis methods, characterization routes and applications towards drugs, J. Environ. Anal. Toxicol. 6 (2016) 1–10.
[39] J. Liu, Adsorption of DNA onto gold nanoparticles and graphene oxide: surface science and applications, Phys. Chem. Chem. Phys. 14 (2012) 10485–10496.
[40] J. Liu, W. Bai, S. Niu, C. Zhu, S. Yang, A. Chen, Highly sensitive colorimetric detection of 17β-estradiol using split DNA aptamers immobilized on unmodified gold nanoparticles, Sci. Rep. 4 (2014) 1–6.
[41] S. Wang, S. Gao, S. Sun, Y. Yang, Y. Zhang, J. Liu, Y. Dong, H. Su, T. Tan, A molecular recognition assisted colorimetric aptasensor for tetracycline, RSC Adv. 6 (2016) 45645–45651.
[42] Z. Chen, J. Guo, H. Ma, T. Zhou, X. Li, A simple colorimetric sensor for potassium ion based on DNA G-quadruplex conformation and salt-induced gold nanoparticles aggregation, Anal. Methods 6 (2014) 8018–8021.
[43] H. Li, L. Rothberg, Colorimetric detection of DNA sequences based on electrostatic interactions with unmodified gold nanoparticles, Proc. Natl. Acad. Sci. U. S. A. 101 (2004) 14036–14039.
[44] N.P. Pai, C. Vadnais, C. Denkinger, N. Engel, M. Pai, Point-of-care testing for infectious diseases: diversity, complexity, and barriers in low- and middle-income countries, PLoS Med. 9 (2012) 1–7.
[45] Y. Xu, T. Han, X. Li, L. Sun, Y. Zhang, Y. Zhang, Colorimetric detection of kanamycin based on analyte-protected silver nanoparticles and aptamer-selective sensing mechanism, Anal. Chim. Acta 891 (2015) 298–303.
[46] S. Niu, Z. Lv, J. Liu, W. Bai, S. Yang, A. Chen, Colorimetric aptasensor using unmodified gold nanoparticles for homogeneous multiplex detection, PLoS One 9 (2014) 1–6.